MECHANISM OF MERCURY PERMEATION THROUGH LIQUID MEMBRANE CONTAINING DICYCLOHEXYL-24-CROWN-8

TAKESHI KATAOKA, TADAAKI NISHIKI
AND MASAO YAMAUCHI
Department of Chemical Engineering, University of Osaka Prefecture, Sakai 591

Key Words: Liquid Membrane, Permeation Mechanism, Mercury, Crown Ether, Extraction

The permeation mechanism of mercury was studied, using a newly devised three-liquid phase contact apparatus with flat interfaces. It is possible by using the apparatus for a feed, membrane and stripping solutions to contact in a similar manner as in the liquid membrane technique. Mercury in the feed phase permeates through the membrane phase of xylene solution of dicyclohexyl-24-crown-8 (C-24) to the stripping phase of sodium chloride solution. The permeation rate of mercury can be explained by a permeation model which takes account of the dissolution of mercury to the membrane phase and the interfacial reaction between mercury and C-24, in addition to the diffusion processes in the aqueous film and the membrane phase.

Introduction

The recovery of mercury from aqueous solutions is of practical importance from the viewpoint of the recycling of industrial resources and wastewater treatment. The liquid-liquid extraction equilibrium of mercury by dicyclohexyl-24-crown-8 (C-24) has been investigated by the authors.[2] The results suggested the potential for using the liquid membrane technique, in which C-24 and an aqueous sodium chloride solution are used as a carrier and a stripping solution, respectively, to separate and concentrate mercury.

In the practical application of the liquid membrane technique, it is necessary to clear the mass transfer mechanism for permeation through the liquid membrane. A new three-liquid phase contact apparatus for the elucidation of the permeation mechanism was devised. It is possible that feed, membrane and stripping solutions contact in a similar manner as in the liquid membrane technique without the use of surfactant or supported solid membrane. The apparatus has the advantage that the membrane phase can be remarkably thinned and a definite flow in the membrane phase may be probably formed in comparison with conventional bulk liquid membranes. It may be considered, therefore, to be appropriate for the study of the permeation mechanism and the effect of surfactant on the permeation rate.

In this work, adopting the apparatus, the permeation mechanism of mercury has been studied, using a xylene solution of C-24 as a liquid membrane solution in the absence of surfactant. The characteristics of the apparatus have been also examined by the extraction of hydrochloric acid by a high-molecular weight amine.

Received May 8, 1986. Correspondence concerning this article should be addressed to T. Nishiki. M. Yamauchi is now with Nippon Steel Co., Ltd., Sakai 590.

1. Experimental

1.1 Apparatus

The three-liquid phase contact apparatus with flat interfaces is schematically shown in **Fig. 1**. The apparatus is constructed of three glass cells, F, S and M. Cells F and S are two forked glass cells each equipped with four baffle plates. Cell M can be made by clamping a Viton packing between the two forked cells and the cover, and therefore it has a space nearly equal to the thickness of the packing. An aqueous mercury chloride solution (feed phase III), aqueous sodium chloride solution (stripping phase I) and xylene solution of C-24 (membrane phase II) are supplied in cells F, S and M, respectively. Packing of 1 mm thickness was used in this study, though the thickness of the membrane phase can be varied freely by changing the thickness of the packing. Hence, the volume of membrane phase was $9.3\times10^{-6}\,m^3$ and that of the solution in cells F and S was $2.6\times10^{-4}m^3$. The interfacial contact areas between cells F and M and cells S and M were 2.38×10^{-3} and $2.37\times10^{-3}m^2$, respectively. Agitation was carried out at $2.5\,s^{-1}$ by using stirring rods fitted at three points with twin flat blades in cells F and S. The apparatus was placed in an air bath which was maintained at 298 K.

1.2 Procedure

The aqueous solutions were supplied up to a constant level in cells F and S. The stirrers were started as soon as a known volume of xylene solution was carefully supplied from the top of the cover without disturbing the interfaces. Adding the original aqueous solutions into each cell to maintain the initial levels of

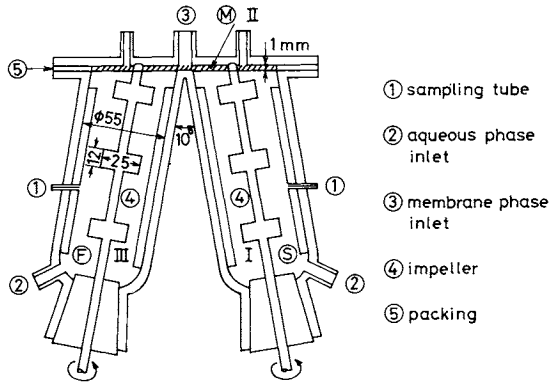

Fig. 1. Three-liquid phase contact apparatus with flat interfaces.

the interfaces, about $5.5\times10^{-6}\,m^3$ of samples were taken with a syringe from each cell at regular time intervals. The mercury concentrations of the samples were determined by chelate titration.

For the experiment of extraction alone, the aqueous $HgCl_2$ solution was supplied in cells F and S and the xylene solution of C-24 was filled in cell M. Mercury was extracted through interfaces F-M and S-M. In the stripping experiment the aqueous NaCl solution was supplied in cells F and S, and the xylene solution of C-24 loaded mercury was supplied in cell M.

2. Permeation Model

When the three phases are in contact as in the present experiment, mercury of feed phase III permeates through membrane phase II into stripping phase I. For such a permeation process the following model may be considered. The bulk phases III and I are stirred sufficiently. Phase II moves due to the stirring of phases III and I. The flow behaviour was observed to be a circulating flow as shown in **Fig. 2**(a) because the stirrers in phases III and I were rotated in the same direction. The figure also describes the plane at which the phase II contacts phases III and I in the apparatus. The flow is simplified through (b) to (c). Furthermore, since the thickness δ of the II phase is thin, it is assumed that the laminar velocity distribution as described in (d) is formed on the two phase contact interfaces ($x_{e0}\sim x_{e1}$, $x_{s0}\sim x_{s1}$) and broken down in the regions ($x_{e1}\sim x_{s0}$, $x_{s1}\sim x_{e0}$) where the lower side of phase II contacts solid planes. Therefore, at the III–II interface ($x_{e0}\sim x_{e1}$) mercury chloride (A) is extracted to the II phase by both dissolution and complex formation with C-24 (B) expressed by the following equation:[2]

$$A+\bar{B}\rightleftarrows\overline{AB} \tag{1}$$

and at the I–II interface ($x_{s0}\sim x_{s1}$) free mercury chloride ($\bar{A}$) and the mercury complex ($\overline{AB}$) are stripped to phase I. Mercury in phase III can be

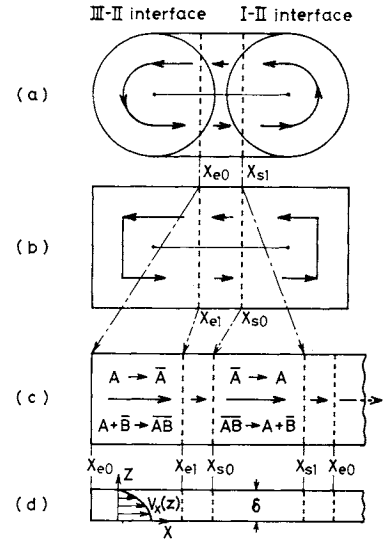

Fig. 2. Permeation model.

permeated and concentrated into phase I by repeating this process.

When it is assumed that the solutes in phase II are transported in the x-direction by the flow and in the z-direction by molecular diffusion, and that the reaction of complex formation occurs only at the interface, the following equation is obtained from the mass balance.

$$\bar{D}_j(\partial^2\bar{C}_j/\partial z^2)=V_x(z)(\partial\bar{C}_j/\partial x) \tag{2}$$

Here the subscript j represents the components A, B and AB, and $V_x(z)$ is the velocity distribution given by

$$V_x(z)=V_i\{1-(z/\delta)^2\} \tag{3}$$

The boundary conditions are expressed as follows:

$$x=x_{e0},\,x_{s0}\quad;\quad \bar{C}_j=\bar{C}_{j0}=\bar{C}_{javg}\big|_{x=x_{s1},\,x_{e1}} \tag{4}$$

$$z=0\quad;\quad \bar{D}_j(\partial\bar{C}_j/\partial z)=-r_j,\quad j=B,\,AB \tag{5}$$

$$(x_{e0}\le x\le x_{e1});\quad -\bar{D}_A(\partial\bar{C}_{Ae}/\partial z)=k_s(C^i_{AIII}-\bar{C}^i_{Ae}) \tag{6}$$

$$(x_{s0}\le x\le x_{s1});\quad -\bar{D}_A(\partial\bar{C}_{As}/\partial z)=k_s(\bar{C}^i_{As}-C^i_{AI}) \tag{7}$$

$$z=\delta\quad;\quad \partial\bar{C}_j/\partial z=0 \tag{8}$$

Equation (4) shows that the concentration distribution formed on each interface is averaged by the breakdown of the velocity distribution, and the fluid of uniform concentration enters the next area, forming a two-phase interface. Equations (6) and (7) express the interfacial resistance to the transfer of free mercury chloride, and the mass transfer coefficient k_s at the interface is assumed not to change in regions III–II and I–II. r_j is the reaction rate at the interface, and the superscript i denotes the interface.

The interfacial reaction described in Eq. (1) is modelled as shown in **Fig. 3** since B and AB are interfacially active.[5] That is, at the III–II interface the reaction may be considered to proceed along the following three steps: ① adsorption of B to the

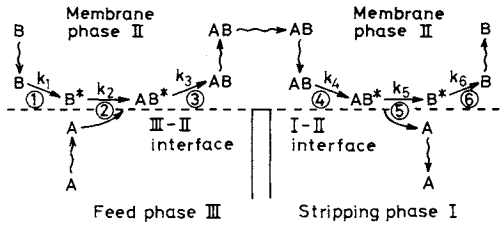

Fig. 3. Interfacial reaction model.

interface, ② complex formation between adsorbed species B^* and A in phase III, and ③ desorption of product AB^* to phase II. The rate for each step is expressed as follows:

$$r_1 = k_1 \bar{C}^i_B \theta_V - k_{-1}\theta_B = k_1 \bar{C}^i_B \theta_V - (k_1/K_1)\theta_B \quad (9)$$

$$r_2 = k_2 C^i_A \theta_B - k_{-2}\theta_{AB} = k_2 C^i_A \theta_B - (k_2/K_2)\theta_{AB} \quad (10)$$

$$r_3 = k_3 \theta_{AB} - k_{-3}\bar{C}^i_{AB}\theta_V = k_3\theta_{AB} - (k_3/K_3)\bar{C}^i_{AB}\theta_V \quad (11)$$

From these equations and the relations represented by Eqs. (12) and (13), the reaction rate is given by Eq. (14) (see **Appendix**).

$$\theta_V + \theta_B + \theta_{AB} = 1 \quad (12)$$

$$r = r_1 = r_2 = r_3 \quad (13)$$

$$r = \frac{k_1 k_2 k_3 (C^i_A \bar{C}^i_B - \bar{C}^i_{AB}/K)}{(k_1 \bar{C}^i_B + k_3 + k_3 \bar{C}^i_{AB}/K_3)(k_1/K_1 + k_2 C^i_A + k_2/K_2) - (k_1 \bar{C}^i_B - k_2/K_2)(k_1/K_1 - k_3)} \quad (14)$$

Here

$$K = K_1 K_2 K_3$$

On the other hand, the reaction rate at the I–II interface is derived similarly by taking into account the following reaction steps: ④ adsorption of AB to the interface, ⑤ dissociative reaction of AB^* to A and B^*, and ⑥ desorption of B^* to phase II.

The fluxes in the aqueous films of phases III and I, respectively, are given by

$$J_{III} = k_w(C_{AIII} - C^i_{AIII}) \quad (15)$$

$$J_I = k_w(C^i_{AI} - C_{AI}) \quad (16)$$

where k_w is the mass transfer coefficient in the aqueous film.

Consequently, if the values of V_i, k_s and k_w are given and the reaction rate is evaluated from Eq. (14), the change of mercury concentration with time can be calculated by using Eqs. (2) to (8), (15) and (16).

3. Results and Discussion

3.1 Extraction of hydrochloric acid by Amberlyte LA-II

To investigate the model's applicability, variations of HCl concentration with time were measured using several HCl solutions as phases III and I and a xylene solution of 157 mol/m^3 Amberlyte LA-II as phase II. The concentration change in phase III agreed with that in phase I and is shown in **Fig. 4**. In this system, the extraction mechanism has been clarified;[4] that is, hydrochloric acid reacts instantaneously with LA-II at the interface and is extracted into the membrane phase as an amine-hydrochloric acid salt.

When the initial HCl concentration C^0_{HCl} is high, such as 88 and 127 mol/m^3, the extraction rate is not affected by C^0_{HCl} because the amine is thoroughly transformed to the amine salt at the interface and the diffusion of the amine salt in the membrane phase is the rate-controlling step. The extraction rates by the model were calculated for various V_i values by using the diffusivity of amine salt estimated from the Wilke-Chang equation. As is clear from the figure, the solid line for the V_i value of 8.7×10^{-3} m/s is in good agreement with the observed results. In the region of C^0_{HCl} less than 40 mol/m^3 the extraction rate decreases with decreasing C^0_{HCl} due to the effect of the diffusional resistance in the aqueous film in addition to the membrane phase diffusion. The solid lines below $C^0_{HCl} = 40$ mol/m^3 are the results calculated by considering both resistances, and by using the k_w value of 4.0×10^{-5} m/s and the relation of extraction equilibrium.[3] They agree with the observed values at every HCl concentration. Consequently, it became clear that the above model can be satisfactorily applied. The aqueous film thickness of 8.5×10^{-5} m obtained from the diffusivity of HCl[1] and k_w, and the value of V_i represented in Fig. 4 were used in the subsequent calculations.

3.2 Extraction rate of mercury

The extraction rates of mercury were measured by varying the initial Hg concentration C^0_A at C-24 concentrations $\bar{C}_{BT}$ of 10 and 20 mol/m^3, respectively. The result for $\bar{C}_{BT} = 20$ mol/m^3 is shown in **Fig. 5**. The solid lines in the figure are the results calculated from the model. In this calculation, the k_w value of 1.3×10^{-5} m/s, which was obtained from the diffusivity of mercury chloride of 1.12×10^{-9} m^2/s[6] and the aqueous film thickness described above, was used. The value of k_s was obtained as 2.2×10^{-7} m/s from the result of a permeation experiment discussed later. Furthermore, the following equation was adopted as the interfacial reaction rate and the k_1 value of 1.5 m/s was used.

$$r = \frac{k_1(\bar{C}^i_B - \bar{C}^i_{AB}/KC^i_A)}{1 + (\bar{C}^i_{AB}/K_2K_3C^i_A) + (\bar{C}^i_{AB}/K_3)} \quad (17)$$

It was derived from Eq. (14) by assuming that the

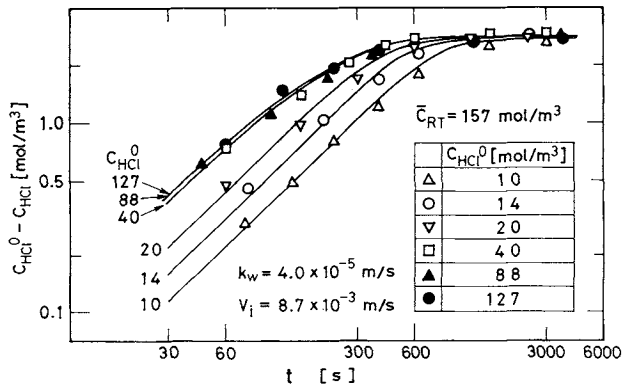

Fig. 4. Extraction rate of hydrochloric acid by Amberlyte LA-II.

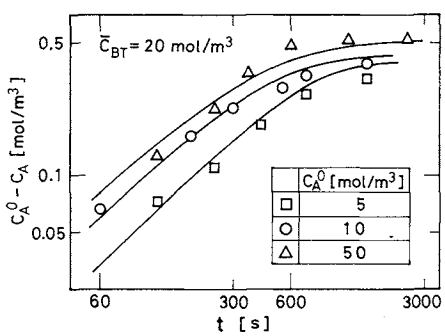

Fig. 5. Effect of initial mercury concentration on extraction rate of mercury.

adsorption rate of B is very slow in comparison with the other rates in the reaction steps. The values of K_1 and K_3 were obtained in the previous study,[5] and therefore K_2 was determined at 0.581 m³/mol from K of 1.90 m³/mol in the equilibrium relation of mercury extraction.[2] These constants are summarized in **Table 1**.

The calculated results are in good agreement with the observed values for every C_A^0 value.* Similar results were obtained for $\bar{C}_{BT}$ of 10 mol/m³.

Figure 6 shows the extraction rates measured by varying $\bar{C}_{BT}$ at $C_A^0 = 50$ mol/m³. The results calculated in the same way as in the case of Fig. 5 are represented by the solid lines and also agree with the observed values.

3.3 Stripping rate of mercury

When the adsorption rate of the complex AB to the interface among the reaction steps may be assumed to be very slow compared with the other steps at the stripping interface, the disappearance rate of AB is derived in a similar manner as Eq. (17).

$$-r = \frac{(k_4/K_4)(KC_A^i\bar{C}_B^i - \bar{C}_{AB}^i)}{1 + K_5K_6C_A^i\bar{C}_B^i + K_6\bar{C}_B^i} \qquad (18)$$

* The calculations were similarly performed by assuming that the step ② or ③ is the rate-controlling step. However, agreement between calculated and experimental results was not obtained.

Table 1. Mass transfer coefficient, reaction rate constant and equilibrium constant

$k_w = 1.3 \times 10^{-5}$ m/s,	$k_5 = 2.2 \times 10^{-7}$ m/s
$k_1 = 1.5$ m/s,	$k_4 = 2.0 \times 10^{-5}$ mol/(m²·s)
$K = 1.90$ m³/mol	
$K_1 = 11.9$ m³/mol,	$K_4 = 1.94$ mol/m³
$K_2 = 0.581$ m³/mol,	$K_5 = 0.581$ m³/mol
$K_3 = 0.275$ mol/m³,	$K_6 = 1.69$ m³/mol

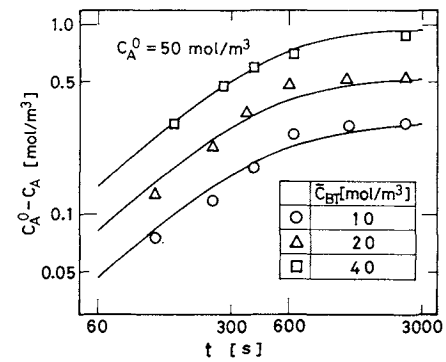

Fig. 6. Effect of C-24 concentration on extraction rate of mercury.

Here

$$K = K_4K_5K_6$$

The value of K_4 is calculated from the K_6 value reported in the previous paper[5] by assuming that K_5 is equal to K_2. These equilibrium constants are also represented in Table 1.

The stripping rates were measured by use of the membrane phases loaded mercury at different concentrations and the aqueous phase of 1 kmol/m³ NaCl. The results are shown in **Fig. 7**. The solid lines are the stripping rates calculated by using Eq. (18) with the rate constant k_4 of 2.0×10^{-5} mol/(m²·s). Agreement between calculated and experimental results is fairly good. A similar result was obtained for a NaCl concentration of 2 kmol/m³.

Calculations from the model in which the interfacial reaction is controlled by step ⑥ were also carried out, but the observed results could not be explained by the model. Thus, the rate-controlling step at the stripping interface is different from that at the extractive interface. This may be due to a difference between the aqueous phases.

3.4 Permeation rate of mercury

Mercury was made to permeate through phase II containing 10 mol/m³ C-24 from the $HgCl_2$ solution of phase III into the 1 kmol/m³ NaCl solution of phase I. **Figure 8** shows the decrease of mercury concentration with time in phase III and the increase in phase I. The permeation rate can be calculated by taking into account both the extraction and the stripping processes and by using the parameters obtained for the respective process. In the figure the

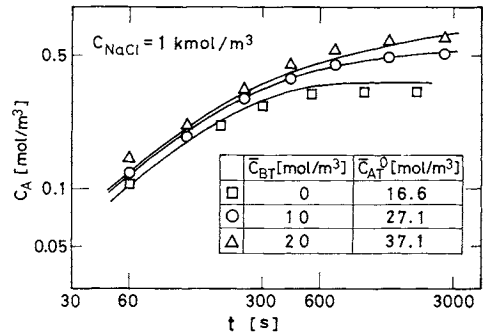

Fig. 7. Stripping rate of mercury.

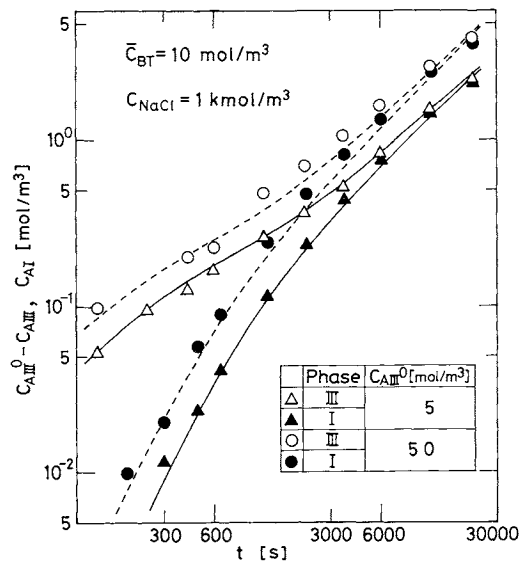

Fig. 8. Effect of initial mercury concentration on permeation rate of mercury.

solid and broken lines are the calculated results for C_{AIII}^0 of 5 and 50 mol/m³, respectively. They are in satisfactory agreement with the observed values.

Figure 9 shows the results measured by varying $\bar{C}_{BT}$ at $C_{AIII}^0 = 10$ mol/m³. When the value of $\bar{C}_{BT}$ is 0, that is, when the membrane solution consists only of xylene, mercury permeates only by means of dissolution. The dotted-broken lines in the figure are the permeation rates calculated by using the k_s value of 2.2×10^{-7} m/s described above. They agree with the experimental data, indicating that the value of k_s is appropriate for evaluating the interfacial resistance to the dissolution of mercury chloride. The solid and broken lines are the calculated results for $\bar{C}_{BT}$ of 10 and 40 mol/m³, respectively, and they are in satisfactory agreement with the observed results.

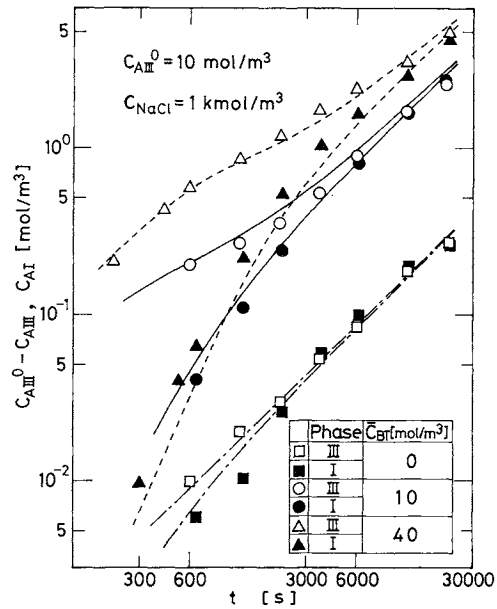

Fig. 9. Effect of C-24 concentration on permeation rate of mercury.

Conclusion

The permeation mechanism of mercury was studied using a three-liquid phase contact apparatus with flat interfaces. Mercury was permeated through the xylene solution of C-24 of the membrane phase from the aqueous mercury chloride solution of the feed phase into the aqueous sodium chloride solution of the stripping phase.

The permeation rate can be interpreted by the permeation model, taking into account the interfacial reaction mechanism which was derived on the basis of the results for the extraction equilibrium and the interfacial adsorption equilibrium, and the diffusion process in the membrane phase. The interfacial reaction at the extractive interface and that at the stripping interface are controlled by the adsorption steps of C-24 and the mercury-C-24 complex, respectively.

Appendix

The following equation is derived from Eqs. (9), (10), (12) and (13).

$$(k_1\bar{C}_B^i - k_2/K_2)\theta_V = (k_1/K_1 + k_2 C_A^i + k_2/K_2)\theta_B - k_2/K_2 \qquad \text{(A-1)}$$

A similar relation between θ_V and θ_B is obtained from Eqs. (9), (11), (12) and (13).

$$(k_1\bar{C}_B^i + k_3 + k_3\bar{C}_{AB}^i/K_3)\theta_V = (k_1/K_1 - k_3)\theta_B + k_3 \qquad \text{(A-2)}$$

From Eqs. (A-1) and (A-2), θ_V and θ_B are expressed as follows:

$$\theta_V = \frac{k_2k_3C_A^i + k_1k_3/K_1 + k_1k_2/K_1K_2}{(k_1\bar{C}_B^i + k_3 + k_3\bar{C}_{AB}^i/K_3)(k_1/K_1 + k_2C_A^i + k_2/K_2) - (k_1\bar{C}_B^i - k_2/K_2)(k_1/K_1 - k_3)} \qquad \text{(A-3)}$$

$$\theta_B = \frac{k_1k_3\bar{C}_B^i + k_1k_2\bar{C}_B^i/K_2 + k_2k_3\bar{C}_{AB}^i/K_2K_3}{(k_1\bar{C}_B^i + k_3 + k_3\bar{C}_{AB}^i/K_3)(k_1/K_1 + k_2C_A^i + k_2/K_2) - (k_1\bar{C}_B^i - k_2/K_2)(k_1/K_1 - k_3)} \qquad \text{(A-4)}$$

Substituting Eqs. (A-3) and (A-4) in Eq. (9) yields Eq. (14).

Nomenclature

C	=	concentration	$[mol/m^3]$
D	=	diffusivity	$[m^2/s]$
J	=	flux	$[mol/(m^2 \cdot s)]$
K	=	equilibrium constant of mercury extraction	$[m^3/mol]$
K_{1-6}	=	equilibrium constants of each reaction step ① to ⑥	$[m^3/mol], [mol/m^3]$
k_s	=	mass transfer coefficient at interface	[m/s]
k_w	=	mass transfer coefficient in aqueous film	[m/s]
k_1, k_{-1}	=	adsorption rate constants of step ①	$[m/s], [mol/(m^2 \cdot s)]$
k_2, k_{-2}	=	reaction rate constants of step ②	$[m/s], [mol/(m^2 \cdot s)]$
k_3, k_{-3}	=	desorption rate constants of step ③	$[mol/(m^2 \cdot s)], [m/s]$
k_4	=	adsorption rate constant of step ④	$[mol/(m^2 \cdot s)]$
r	=	reaction rate at interface	$[mol/(m^2 \cdot s)]$
t	=	contact time	[s]
V_i	=	velocity at interface	[m/s]
V_x	=	velocity in x-direction	[m/s]
x	=	coordinate along interface	[m]
z	=	vertical coordinate to interface	[m]
δ	=	thickness of membrane phase	[m]
θ_j	=	fraction of interfacial area occupied by species j	[—]

〈Subscripts〉

A	=	mercury
AB	=	mercury-C-24 complex
B	=	C-24
e	=	extraction area
j	=	chemical species
R	=	Amberlyte LA-II
s	=	stripping area
T	=	total
I	=	stripping phase
II	=	membrane phase
III	=	feed phase

〈Superscripts〉

i	=	interface
0	=	initial
$^-$	=	membrane phase
*	=	adsorption state at interface

Literature Cited

1) Chang, P. and C. R. Wilke: *J. Phys. Chem.*, **59**, 592 (1955).
2) Kataoka, T., T. Nishiki, T. Sasaki and D. Kato: *J. Chem. Eng. Japan*, **16**, 459 (1983).
3) Kataoka, T., T. Nishiki, Y. Tamura and K. Ueyama: *J. Chem. Eng. Japan*, **13**, 35 (1980).
4) Kataoka, T., T. Nishiki and K. Ueyama: *Chem. Eng. J.*, **10**, 189 (1975).
5) Kataoka, T., T. Nishiki and M. Yamauchi: *J. Chem. Eng. Japan*, **19**, 147 (1986).
6) Washburn, E. W. (ed.): "International Critical Tables," Vol. 5, p. 65, McGraw-Hill, New York (1929).